Lifelong Exercise in Age Rats Improves Skeletal Muscle Function and MicroRNA Profile

HAO-EN GAO, FANG-HUI LI, TIAN XIE, SONG MA, YI-BO QIAO, DA-SHUAI WU, and LEI SUN

School of Sport Sciences, Nanjing Normal University, Nanjing, CHINA

ABSTRACT

GAO, H.-E., F.-H. LI, T. XIE, S. MA, Y.-B. QIAO, D.-S. WU, AND L. SUN. Lifelong Exercise in Age Rats Improves Skeletal Muscle Function and MicroRNA Profile. *Med. Sci. Sports Exerc.*, Vol. 53, No. 9, pp. 1873–1882, 2021. **Purpose:** Lifelong exercise is known to attenuate sarcopenia (age-associated reduction in muscle mass and function); however, the underlying molecular mechanisms remain unclear. As microRNAs are widely involved in the regulation of skeletal muscle growth and development, we aimed to evaluate the effects of lifelong regular exercise on age-related alterations in muscle microRNA expression profiles as well as on skeletal muscle atrophy, apoptosis, and mitochondria and autophagy dysfunction. **Methods:** Female 8-month-old Sprague-Dawley rats were divided into four groups; 1) 18 months of moderate-intensity continuous training (MICT) initiated at 8 months (adult-MICT, $n = 12$), 2) 8 months of MICT initiated at 18 months (presarcopenia-MICT, $n = 12$), 3) 8-month-old adult sedentary controls (adult-SED), and 4) 26-month-old aging sedentary controls (old-SED). Age skeletal muscles were then subjected to quantitative reverse transcription–polymerase chain reaction, Kyoto Encyclopedia of Genes and Genomes, immunoblotting, and miR-486 3′ untranslated region luciferase reporter gene analyses. **Results:** Age-related loss of miR-486 expression was improved, skeletal muscle atrophy and apoptosis were downregulated, and mitochondrial activity and autophagy were upregulated in the adult-MICT group. Kyoto Encyclopedia of Genes and Genomes analysis revealed that the PI3K/Akt pathway was upregulated in adult-MICT rats compared with that in old-SED. *In vitro* analyses in rat skeletal muscle L6 cells further confirmed that miR-486 targets PTEN, not SAV1, thereby activating the PI3K/Akt pathway and indirectly inhibiting HIPPO signaling. **Conclusions:** Compared with presarcopenia-MICT rats, adult-MICT rats experienced greater beneficial effects regarding ameliorated age-related alterations in muscle miRNA expression profile, skeletal muscle atrophy, apoptosis, and mitochondria and autophagy dysfunction, which is potentially associated with the increased miR-486 expression and concomitant targeting of the PTEN/Akt signaling pathway. **Key Words:** LIFELONG EXERCISE, SARCOPENIA, MIR-486, AKT

Sarcopenia, the age-related attenuation of skeletal muscle mass, represents a major problem in aging populations and leads to metabolic disorders, increases the risk of cardiovascular disease and disability, and significantly reduces quality of life (1). Drivers of sarcopenia include decreased autophagy and mitochondrial biosynthesis as well as attenuated regenerative capacity, oxidative stress, ubiquitin–proteasome activation, and myocyte apoptosis (2). Previous studies have shown that lifelong regular exercise is associated with maintenance of muscle mass, reduced adipose tissue infiltration, and upregulated expression of sirtuin-3 (SIRT3) and superoxide dismutase 2 (SOD2) in the vastus lateralis muscle of the elderly, thereby improving skeletal muscle resilience to unaccustomed loading and adaptability in adult life (3–6). Moreover, lifelong regular exercise affects methylation of skeletal muscle genes related to energy metabolism and myogenesis (7), attenuates age-related decline in mitochondrial content and function, and attenuates dysfunction of autophagy-mediated degradation (8,9). We previously demonstrated that exercise initiated during adulthood may assist in countering age-induced poor physical functioning and chronic low-grade inflammatory status by increasing the abundance of phosphorylated protein kinase B (p-Akt) and downstream phosphorylated forkhead box O1 (p-FoxO1) protein in rat skeletal muscle cells (10). However, the specific mechanism underlying the prevention of sarcopenia development by the Akt/FoxO1 pathway in these animals remains unknown.

MicroRNAs (miRNAs) are small, noncoding, single-stranded RNAs (approximately 21–25 nucleotides) that promote target

mRNA degradation and translation termination by base pairing with the 3′ untranslated region of the target gene, thus contributing to the regulation of cell function at the transcriptional level (11,12). Indeed, specific miRNAs are reportedly involved in the regulation of skeletal muscle growth and development, including miR-1, miR-133, miR-486, miR-206, and miR-499, which are identified as muscle miRNAs (myomiRs) as they are specifically or highly expressed in muscle tissue (11,12). MiR-1, miR-133a, miR-133c, miR-182, miR-126, miR-23a, miR-486, and miR-19a may revert skeletal muscle loss by downregulating the expression of muscle atrophy F-box (MAFbx) and ring finger 1 (MuRF1) (11,13,14); contrastingly, upregulation of miR-208b, miR-499, miR-628, miR-21, and miR-206 may accelerate muscle loss in aging skeletal muscle (11,15). Moreover, regular exercise significantly increases the baseline expression of miR-486, miR-215, and miR-941, and decreases that of miR-151b in older individuals (16). However, little is known regarding the impact of such altered miRNA expression on the regulation of muscle atrophy and function in individuals who initiated regular exercise regimens in adulthood compared with those who started exercising later in life.

Therefore, in this study, we evaluated the effects of lifelong regular exercise on age-related alterations in myomiR expression profiles and associated skeletal muscle phenotypes. To this end, we compared rats exposed to long-term moderate-intensity continuous training (MICT) initiated at 8 months with those whose MICT was initiated at 18 months (presarcopenia-MICT) until 26 months of age. Moreover, we performed myomiR expression profiling and Kyoto Encyclopedia of Genes and Genomes (KEGG) enrichment analysis of aging- and exercise-associated genes to investigate the potential mechanisms underlying the lifelong exercise-associated prevention of sarcopenia.

METHODS

Animals. Sprague-Dawley rats (8 months old) were purchased from Guangdong Medical Laboratory Animal Center (Foshan, Guangdong, China). The rats were maintained on an artificial 12-h light–dark cycle (6:00 AM–6:00 PM) at constant room temperature ($23°C \pm 1°C$) in the Laboratory Animal Center, School of Sports Science and Physical Education, South China Normal University. The animals were housed in their respective groups in a collective cage and were provided with standard laboratory chow (56.8% carbohydrate, 22.5% protein, 3.5% lipids, and 17.2% other nutrients) and water *ad libitum*. Every possible effort was made to minimize both the number and suffering of animals, according to the principles of the Declaration of Helsinki, and the protocols were approved by the Animal Experiment Ethical Inspection Form of Nanjing Normal University (IACUU-1903006).

After 1 wk of preconditioning feeding, 8-month-old rats ($n = 12$) were randomly selected to represent the adult sedentary (adult-SED) group and were sacrificed via intraperitoneal injection of pentobarbital sodium ($50 \ mg \cdot kg^{-1}$ body weight).

The remaining animals were randomly divided into three groups as follows: 1) 18-month MICT initiated at 8 months of age (adult-MICT, $n = 12$), 2) 8-month MICT initiated at 18 months of age (presarcopenia-MICT, $n = 12$) until 26 months (sarcopenia) (10), and 3) 26-month-old rats representing age sedentary animals (old-SED, $n = 12$). Rats in the old-SED group were handled in an identical manner as the MICT groups; however, they did not participate in any exercise treatment for the 18-month duration of the experiment. During the experiment, six rats were excluded from the study: four presarcopenia-MICT rats (of which two died from causes unrelated to exercise and two from severe claw infections) and two old-SED rats (owing to severe eye infections).

Training protocol. All rats were trained over a 2-wk acclimatization course to run on an adapted motor-driven treadmill designed for rats (model FD000043; Flyde Apparatus, Guangzhou, China). During the first week of training, rats were individually placed onto a treadmill lane at a 0° incline for a total of 10 min. At the beginning of the second week of training, rats ran at 10 $m \cdot min^{-1}$ and by the end of the second week, they progressed to 15 $cm \cdot s^{-1}$ at a 0° incline for 30 min. Further details on maximal oxygen uptake ($\dot{V}O_{2max}$) and calculation of training intensity have been previously described (10).

Both exercise protocols included 1 min of warm-up at a constant running speed of 10 $m \cdot min^{-1}$, which corresponded to 35%–40% of $\dot{V}O_{2max}$, followed by 45 min at a constant running speed of 17 $m \cdot min^{-1}$ (corresponding to 75%–80% of $\dot{V}O_{2max}$) and cool-down at a constant running speed of 10 $m \cdot min^{-1}$ for 1 min. To prevent avoidance and ensure exercise training, rats received a light electrical shock (6 mA) if they sat at the base of the treadmill. Within 2 wk of training, the rates of exercise avoidance were minimal and electrical shock was no longer required. Exercise training sessions were held at the same time each morning (10,17).

RNA isolation and quantitative reverse transcription-polymerase chain reaction. The vastus lateralis, which exhibits age-associated decline in mitochondrial biosynthesis and antioxidant systems, ubiquitin–proteasome activation, and myocyte apoptosis, is often used for evaluating sarcopenia-associated alterations in skeletal muscle phenotypes (4). Hence, total RNA was extracted from the vastus lateralis muscle (50 mg) from each rat using TRIzol reagent (1 mL) and thorough grinding using a high-speed tissue grinder. RNA concentration was measured using an ultra-microspectrophotometer (One Drop® 1000+; Thermo Fisher Scientific, Waltham, MA). The prepared RNA (1 µg) was processed using the miRNA 1st Strand cDNA Synthesis Kit (by stem–loop) and HiScript III 1st Strand cDNA Synthesis Kit (+gDNA wiper) for reverse transcription-polymerase chain reaction (RT-PCR; 1880-051; Invitrogen, Carlsbad, CA) to reverse transcribe miRNA and mRNA, respectively, according to the manufacturer's instructions. The synthesized cDNA was further diluted 1:10 in DNase-free water, mixed with the ChamQ SYBR qPCR Master Mix (High ROX Premixed), and analyzed via quantitative RT-PCR using the ABI Step One Plus Real-Time PCR instrument (Foster

City, CA) for 40 cycles. *Gapdh* and U6 served as internal reference genes for mRNA and miRNA, respectively, and the results were calculated using the $2^{-\Delta\Delta Ct}$ method. According to the gene sequences in the NCBI and miRBase databases, the primer sequences of mRNAs, miRNAs, *Gapdh*, and U6 were designed and synthesized by Shanghai Biotech (China); the reverse primer for miRNAs was 5′-AGTGCAGGGTCCGAGGTATT-3′. All other miRNA and related gene primer sequences are listed in Supplemental Table 1 (Appendix, Supplemental Table 1, Primer sequences, http://links.lww.com/MSS/C303).

Identification of miRNA-related signaling pathways. *In silico* identification of molecular pathways potentially affected by the observed alterations in miRNA levels was performed using the web-based computational tool Target Scan 7.1. DIANA-miRPath v3.0 was used to predict miRNA targets from the DIANA-TarBase/DIANA-micro-T-CDS algorithm and combine the results with KEGG analysis to identify possible targets (18). The level of significance was set at $P < 0.01$.

Target prediction and luciferase reporter assay. Using Targetscan and DIANA-TarBase/DIANA-micro-T-CDS, PTEN and Salvador family WW domain containing protein 1 (SAV1) were predicted to be targets of miR-486. Therefore, we synthesized sequences corresponding to both wild type (WT) and mutant (MUT) PTEN and SAV1, which were constructed by Keygenbio (Nanjing, China). Rat skeletal muscle L6 cells were maintained in Dulbecco's modified Eagle medium (Gibco; Thermo Fisher Scientific) supplemented with 10% fetal bovine serum (Gibco), and cultured in a humidified 5% CO_2 incubator at 37°C. According to the manufacturer's instructions, cells were seeded in a 96-well plate 1 d before transfection with pGL3-PTEN-WT, pGL3-PTEN-MUT, pGL3-SAV1-WT, or pGL3-SAV1-MUT (500 ng; Keygenbio), pRL-TK (*Renilla luciferase* normalization control; 50 ng; Promega, Madison, WI), and miR-486 mimic (75 pM; Keygenbio) using Lipofectamine 3000 (Invitrogen); a scrambled sequence was used as a negative control (miR-486 NC; 75 pM; Keygenbio). Cells were collected 48 h after transfection, and luciferase activity was measured using a dual luciferase reporter assay system (Promega).

Western blotting. Cells were seeded in 96-well plates the day before transfection with miR-486 mimic and miR-486 NC (75 pM) using Lipofectamine 3000 according to the manufacturer's instructions. At 48 h after transfection, cells were harvested for Western blot analysis.

L6 cells and vastus lateralis muscle tissue were lysed using radioimmunoprecipitation assay buffer with protease inhibitors, as described previously (10). Total protein (15 μg) was separated using 8%, 10%, and 12% sodium dodecyl sulfate–polyacrylamide gels, and transferred onto a polyvinylidene difluoride membrane. Blots were blocked with 5% skim milk and incubated with the indicated primary antibody overnight at 4°C. The membranes were then incubated with a goat antirabbit peroxidase-conjugated secondary antibody (Santa Cruz Biotechnology, Dallas, TX) for 1 h at approximately 20°C and measured using an infrared imaging system (LI-COR Biosciences, Lincoln, NE). Protein expression was normalized to that of β-actin. All antibodies used for Western blotting are listed in Supplemental Table 1 (Appendix, Supplemental Table 1, Antibodies, http://links.lww.com/MSS/C303).

Statistical analysis. Values were represented as mean ± SD. Before statistical analysis, all data were assessed for normality using the one-sample Kolmogorov–Smirnov test (10). Statistical analysis was performed using GraphPad Prism 7.0 (GraphPad Software Inc., San Diego, CA). According to the variable characteristics, the Student's *t*-test (two-sided) or Mann–Whitney *U* test was used to assess indices of the old-SED and adult-SED rats. The differences in miRNA, mRNA, and protein expression levels among the old-SED, adult-MICT, and presarcopenia-MICT groups were assessed by one-way ANOVA or Kruskal–Wallis *H* tests, depending on whether the variables were normally distributed. CON, miR-486 NC, and miR-486 mimic groups were assessed via one-way ANOVA followed by Tukey's *post hoc* test. *P* values <0.05 were considered statistically significant.

RESULTS

Muscle atrophy, apoptosis, mitochondrial function, and autophagy. We performed Western blotting to determine the expression of protein markers in the vastus lateralis muscle following lifelong exercise. Compared with the adult-SED group, MuRF1, MAFbX, caspase-3, BAX ($P < 0.01$; Fig. 1A), p62, and Beclin-1 ($P < 0.01$; Fig. 1B) levels in the old-SED group were significantly upregulated, whereas those of Bcl-2 ($P < 0.01$; Fig. 1A), SDHA, LC3 II ($P < 0.01$; Fig. 1B), and PGC-1α ($P < 0.05$; Fig. 1B) as well as the Bcl-2/BAX ($P < 0.01$; Fig. 1A) and LC3 II/LC3 I ($P < 0.01$; Fig. 1B) ratios were significantly downregulated. Meanwhile, p70S6K, the Bcl-2/BAX ratio ($P < 0.01$; Fig. 1A), SDHA, PGC-1α, Beclin-1 ($P < 0.01$; Fig. 1B), Bcl-2 ($P < 0.05$; Fig. 1A), COX-IV, and the LC3 II/LC3 I ratio ($P < 0.05$; Fig. 1B) were significantly upregulated, whereas caspase-3 ($P < 0.01$; Fig. 1A) and p62 ($P < 0.05$; Fig. 1B) were significantly downregulated in both the adult-MICT and presarcopenia-MICT groups compared with the old-SED group. Conversely, MuRF1, MAFbx, and BAX ($P < 0.05$; Fig. 1A) levels were significantly decreased, and SIRT3 and LC3 II ($P < 0.05$; Fig. 1B) levels were significantly increased in the adult-MICT group compared with the old-SED group. In addition, p70S6K ($P < 0.01$; Fig. 1A) and LC3 II ($P < 0.01$; Fig. 1B) levels as well as the LC3 II/LC3 I ratio ($P < 0.05$; Fig. 1B) were significantly upregulated, whereas MuRF1, MAFbx ($P < 0.05$; Fig. 1A), p62, and SDHA ($P < 0.01$; Fig. 1B) were significantly downregulated in the adult-MICT group compared with the presarcopenia-MICT group.

Expression of miRNAs and KEGG functional enrichment analysis. We identified 11 differentially expressed miRNAs between the old-SED and adult-SED groups, namely, miR-486, miR-145, miR-133a, miR-19a, and miR-133c, which were significantly downregulated ($P < 0.05$, Fig. 2A), and miR-126, miR-23a ($P < 0.05$, Fig. 2A), miR-182, miR-206, miR-199a, and miR-208b ($P < 0.01$, Fig. 2A), which were
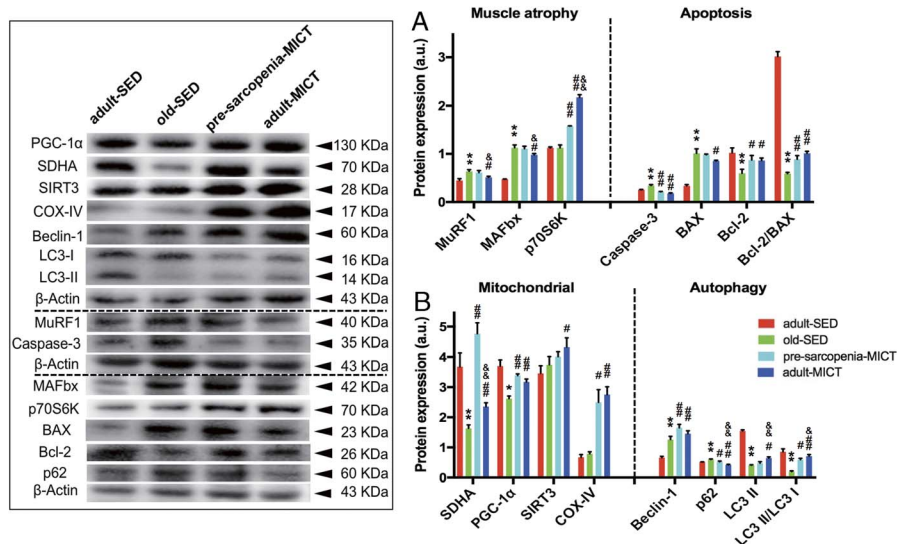
FIGURE 1—Expression of muscle atrophy, apoptosis (A), and mitochondrial function markers as well as autophagy-related proteins (B). Groups: adult-SED, 8 months sedentary; old-SED, 26 months sedentary; adult-MICT, 8 months beginning with moderate-intensity continuous training; and presarcopenia-MICT, 18 months beginning with moderate-intensity continuous training. Training intervention differences among the old-SED, adult-MICT, and presarcopenia-MICT groups were assessed via one-way ANOVA followed by Tukey's *post hoc* test. Age-related differences between the old-SED and adult-SED groups were assessed via independent-samples *t*-tests (two-sided). Values are reported as means ± SD. *$P < 0.05$ and **$P < 0.01$ vs adult-SED; #$P < 0.05$ and ##$P < 0.01$ vs old-SED; &$P < 0.05$ and &&$P < 0.01$ vs presarcopenia-MICT. MuRF1, muscle ring finger 1; MAFbx, muscle atrophy F-box; p70S6K, p70 ribosomal protein S6 kinase; SDHA, succinate dehydrogenase complex subunit A; PGC-1α, peroxisome proliferator-activated receptor γ coactivator-1 α; SIRT3, sirtuin 3; COX-IV, cytochrome c oxidase IV; LC3-II, microtubule-associated protein 1 light chain 3-II.

significantly upregulated. Compared with the old-SED group, miR-23a ($P < 0.01$, Fig. 2A) was significantly downregulated while miR-133a, miR-532, miR-1, miR-208b ($P < 0.05$, Fig. 2A), miR-145, miR-499, miR-19a, and miR-133c ($P < 0.01$, Fig. 2A) were significantly upregulated in the presarcopenia-MICT group. In addition, miR-23a and miR-199a ($P < 0.01$, Fig. 2A) were significantly downregulated, whereas miR-182, miR-486, miR-628, miR-1, miR-208b, miR-499, miR-19a ($P < 0.01$, Fig. 2A), and miR-126 ($P < 0.05$, Fig. 2A) were significantly upregulated in the adult-MICT group compared with the old-SED group. Moreover, miR-182, miR-628, miR-208b ($P < 0.01$, Fig. 2A), miR-126, miR-194, and miR-486 ($P < 0.05$, Fig. 2A) levels were significantly upregulated, whereas those of miR-145, miR-133a, miR-206, miR-199a, and miR-133c ($P < 0.05$, Fig. 2A) were significantly downregulated in the adult-MICT group compared with the presarcopenia-MICT group.

Figures 2B–D shows the KEGG pathway enrichment of differentially expressed miRNAs between the old-SED/adult-SED, adult-MICT/old-SED, and presarcopenia-MICT/old-SED groups. The miRNAs and related downstream genes are listed in Supplemental Table 2 (Appendix, Supplemental Table 2, KEGG-enriched miRNAs and genes, http://links. lww.com/MSS/C304). HIPPO and MAPK signaling pathways were coenriched among the three comparisons, whereas the old-SED/adult-SED and adult-MICT/old-SED differentially expressed miRNAs were specifically enriched in the PI3K/Akt signaling pathway (Figs. 2B, C). Other aging-related pathways were also identified including the neurotrophin, FoxO, and Rap1 pathways in old-SED/adult-SED (Fig. 2B); the Ras, FoxO, Wnt, and Rap1 pathways in adult-MICT/old-SED

(Fig. 2C); and the Wnt and Rap1 pathways in presarcopenia-MICT/old-SED (Fig. 2D).

Expression of HIPPO, MAPK, and PI3K/Akt pathway-related mRNA and proteins. We next determined the mRNA expression of miRNA target genes to further verify the three pathways identified in KEGG analysis (Fig. 3A; Supplemental Figure 1, Changes in mRNA expression of downstream target genes of identified KEGG pathways and expression of HIPPO, MAPK, and PI3K/Akt, http://links.lww.com/MSS/C305). In the old-SED group, Mob1b, Map4k3, and Map4k4 ($P < 0.05$, Fig. 3A) levels were significantly decreased, whereas SAV1 and PTEN ($P < 0.01$, Fig. 3A) levels were significantly increased compared with those in the adult-SED group. Compared with those in the old-SED group, SAV1 and PTEN ($P < 0.05$, Fig. 3A) levels were significantly downregulated in the adult-MICT group, whereas Mapk1 and Map4k3 ($P < 0.01$, Fig. 3A) levels were significantly upregulated in the presarcopenia-MICT group.

The expression of proteins involved in HIPPO, MAPK, and PI3K/Akt signaling was further analyzed using Western blotting. Compared with the adult-SED group, p-LAST1/2, p-YAP ($P < 0.05$, Fig. 3B), and TEAD1 ($P < 0.01$, Fig. 3B) in the old-SED group were significantly upregulated, whereas p-p38 MAPK, p-p38 MAPK/p38 MAPK ratio ($P < 0.01$, Fig. 3C), p-Akt ($P < 0.05$, Fig. 3D), and p-Akt/Akt ratio ($P < 0.01$, Fig. 3D) were significantly downregulated. YAP, p-p38 MAPK, and the p-p38 MAPK/p38 MAPK ratio were significantly upregulated while p-LAST1/2, p-YAP, p-YAP/YAP ratio, and PTEN were significantly downregulated in both the adult-MICT and presarcopenia-MICT groups compared with
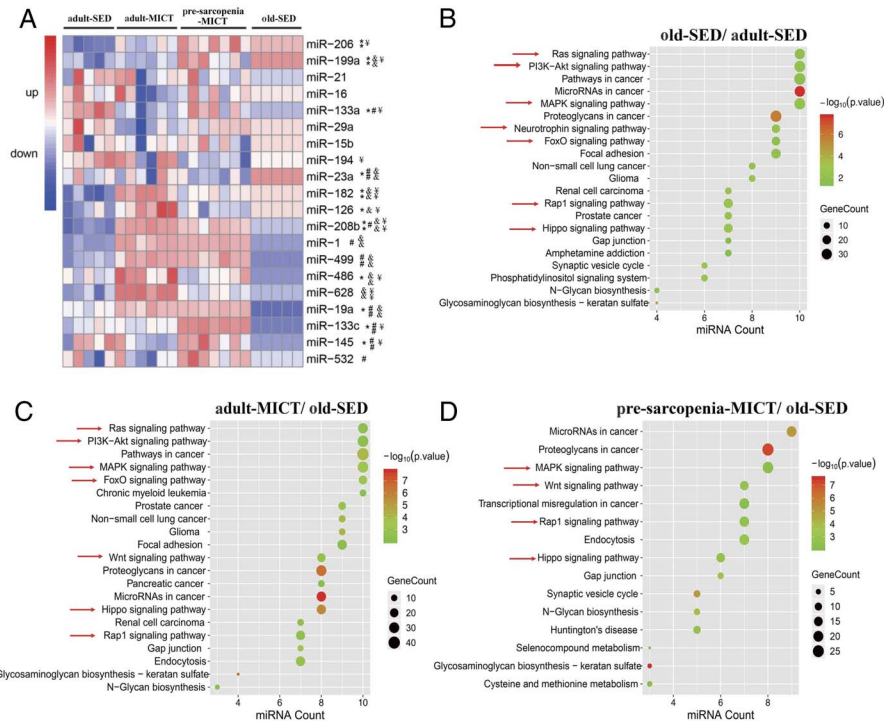
FIGURE 2—Changes in skeletal muscle-associated miRNA expression profiles in rats (A); old-SED/adult-SED (B), adult-MICT/old-SED (C), and presarcopenia-MICT/old-SED differential miRNA enrichment pathways (D). MiRNA count shows the number of differentially expressed miRNAs enriched in the pathway. Groups: adult-SED, 8 months sedentary; old-SED, 26 months sedentary; adult-MICT, 8 months beginning with moderate-intensity continuous training; and presarcopenia-MICT, 18 months beginning with moderate-intensity continuous training. Training intervention differences among the old-SED, adult-MICT, and presarcopenia-MICT groups were assessed via one-way ANOVA followed by Tukey's *post hoc* test or Kruskal–Wallis *H* tests. Age-associated differences between the old-SED and adult-SED groups were assessed via independent-samples *t*-tests (two-sided) or Mann–Whitney *U* test. *$P < 0.05$ and **$P < 0.01$ vs old-SED/adult-SED; #$P < 0.05$ and ##$P < 0.01$ vs presarcopenia-MICT/old-SED; &$P < 0.05$ and &&$P < 0.01$ vs adult-MICT/old-SED; ¥$P < 0.05$ and ¥¥$P < 0.01$ vs adult-MICT/presarcopenia-MICT.

old-SED. Whereas p-MST1/2 ($P < 0.05$, Fig. 3B) was significantly downregulated in the adult-MICT group, TEAD1 ($P < 0.05$, Fig. 3B), p-Akt ($P < 0.01$, Fig. 3D), and the p-Akt/Akt ratio ($P < 0.05$, Fig. 3D) were significantly upregulated compared with that of the old-SED group. In addition, p-MST1/2, p-YAP ($P < 0.05$, Fig. 3B), and PTEN ($P < 0.01$, Fig. 3D) levels were significantly decreased, whereas those of TEAD1 ($P < 0.05$, Fig. 3B), p-p38 MAPK ($P < 0.05$, Fig. 3C), p-p38 MAPK/p38 MAPK ratio ($P < 0.01$, Fig. 3C), p-Akt, and p-Akt/Akt ratio ($P < 0.01$, Fig. 3D) were significantly increased in the adult-MICT group compared with the presarcopenia-MICT group.

MiR-486 directly targets PTEN but not SAV1. The Venn diagram of differentially expressed miRNAs indicated that five miRNAs (miR-628, miR-486, miR-182, miR-126, and miR-199a) were differentially expressed between the adult-MICT and presarcopenia-MICT groups using the old-SED group as a baseline (Fig. 4A). Correlation analysis showed that only miR-486 was significantly negatively correlated with *Sav1* and *Pten* mRNA ($P < 0.05$, Fig. 4B). Furthermore, miR-486 was significantly positively correlated with p-Akt ($P < 0.01$, $r = 0.92$, Fig. 4C), but negatively correlated with p-YAP ($P < 0.05$, $r = -0.68$, Fig. 4E) and showed no relationship with YAP ($P > 0.05$, $r = 0.49$, Fig. 4D).

We next assessed whether the adult-MICT group exhibits inhibited HIPPO and PI3K/Akt signaling via miR-486

targeting of PTEN and SAV1, respectively. Luciferase assays using L6 cells revealed significantly decreased luciferase expression in the PGL3 + PTEN-WT + miR-486-5p group but not the PGL3 + SAV1-WT + miR-486-5p group, indicating that miR-486 can directly target and inhibit PTEN but not SAV1 ($P < 0.01$, Figs. 4F, G).

miR-486 is overexpressed in the HIPPO and PI3K/Akt pathways. Next, the miR-486 mimic and miR-486 NC were added to L6 cells, followed by Western blotting of markers associated with the HIPPO and PI3K/Akt pathway as well as muscle atrophy, apoptosis, and mitochondrial and autophagy. MiR-486 overexpression significantly downregulated p-MST1/2, p-LATS1/2, p-YAP, p-YAP/YAP ratio ($P < 0.01$, Fig. 5A), PTEN ($P < 0.01$, Fig. 5B), MAFbx, MuRF1 ($P < 0.01$, Fig. 5C), caspase-3, BAX ($P < 0.01$, Fig. 5D), and p62 ($P < 0.01$, Fig. 5F), whereas YAP, TEAD1 ($P < 0.01$, Fig. 5A), p-Akt ($P < 0.05$, Fig. 5B), p-Akt/Akt ratio ($P < 0.01$, Fig. 5B), p70S6K ($P < 0.01$, Fig. 5C), Bcl-2, Bcl-2/BAX ratio ($P < 0.01$, Fig. 5D), PGC-1α, SDHA ($P < 0.01$, Fig. 5E), Beclin-1, LC3 II, and LC3 II/LC3 I ratio ($P < 0.01$, Fig. 5F) were significantly upregulated.

DISCUSSION

This study provides mechanistic evidence that differential myomiR expression in skeletal muscle has an important role
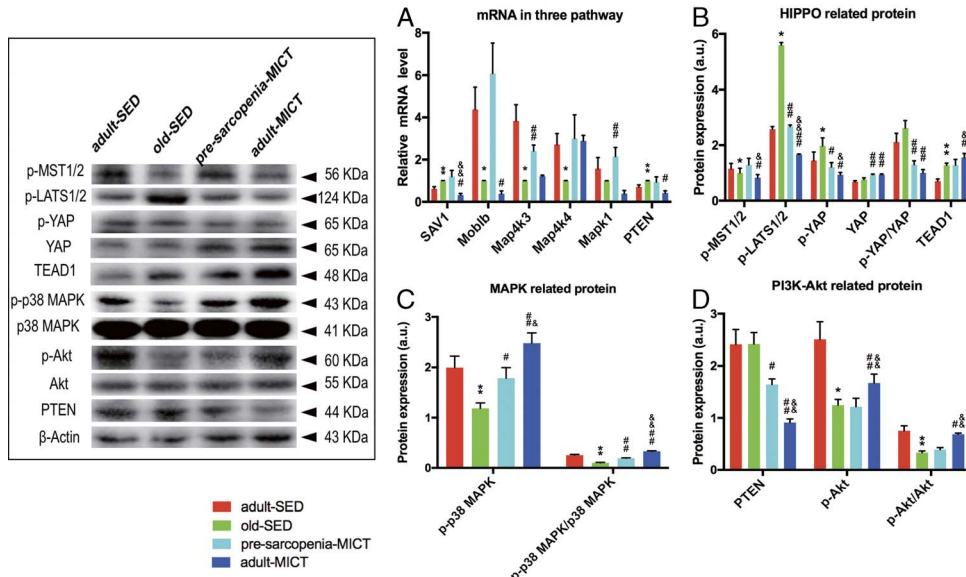
FIGURE 3—Altered mRNA expression of downstream target genes enriched in KEGG pathways, and expression of HIPPO, MAPK, and PI3K/Akt in each study group. Expression of HIPPO, MAPK, and PI3K/Akt-related mRNAs (A). Expression of HIPPO (B), MAPK (C), and PI3K/Akt-related proteins (D). Groups: adult-SED, 8 months sedentary; old-SED, 26 months sedentary; adult-MICT, 8 months beginning with moderate-intensity continuous training; and presarcopenia-MICT, 18 months beginning with moderate-intensity continuous training. Training intervention differences among the old-SED, adult-MICT, and presarcopenia-MICT groups were assessed via one-way ANOVA followed by Tukey's *post hoc* test or Kruskal–Wallis *H* tests. Age-related differences between the old-SED and adult-SED groups were assessed via independent-samples *t*-tests (two-sided) or Mann–Whitney *U* test. Values are reported as means ± SD. $*P < 0.05$ and $**P < 0.01$ vs adult-SED; $\#P < 0.05$ and $\#\#P < 0.01$ vs old-SED; $\&P < 0.05$ and $\&\&P < 0.01$ vs presarcopenia-MICT. p-MST1/2, phosphorylated mammalian ste-20 like kinase 1 and 2; p-LATS1/2, phosphorylated large tumor suppressor kinase 1 and 2; p-YAP, phosphorylated Yes-associated protein; TEAD1, TEA domain transcription factor 1.

in muscle plasticity following lifelong regular exercise initiated earlier in adulthood (adult-MICT) compared with initiation later in life (presarcopenia-MICT), as evaluated in age rats. We showed that aging caused skeletal muscle atrophy, apoptosis, and mitochondrial and autophagy dysfunction as well as altered miRNA expression profiles in skeletal muscle, whereas regular exercise attenuated these effects. We also found that the MAPK pathway was upregulated and HIPPO signaling was downregulated in both exercise groups, whereas PI3K/Akt signaling was specifically upregulated in the adult-MICT group. PTEN and SAV1, members of the PI3K/Akt and HIPPO pathways (19,20), respectively, are targets of miR-486, which exhibited the strongest correlation with p-Akt and p-YAP in the adult-MICT group. Moreover, functional *in vitro* analyses in L6 cells further confirmed that miR-486 targeted PTEN, thereby activating the PI3K/Akt pathway and indirectly inhibiting the HIPPO pathway. Combined, these factors may be related to broader beneficial effects on antiapoptotic factors, mitochondrial function, and autophagy, underlying the attenuated atrophy observed in the age skeletal muscle from the adult-MICT group compared with the presarcopenia-MICT group.

Sarcopenia is accompanied by age-related muscle decline and decreased exercise capacity (1). In the present study, we found that aging was accompanied by downregulation of the Bcl-2/BAX ratio (anti-apoptosis index), PGC-1α and SDHA (mitochondrial function), and p62 and the LC3II/LC3I ratio (autophagy), as well as upregulation of MuRF1 and MAFbx (atrophy). Exercise-induced autophagy, as measured by an

increase in LC3 II and decrease in p62, is reportedly the most effective treatment for maintaining skeletal muscle homeostasis and integrity, improving mitochondrial mass, and slowing sarcopenia (21). Here, both exercise regimens enhanced antiapoptotic protein expression (caspase-3, Bcl-2/BAX ratio), mitochondrial metabolism (SDHA), oxidative energy (COX-IV), and biosynthesis (PGC-1α). The adult-MICT regimen specifically increased autophagic activities (p62, LC3II, LC3II/LC3I ratio), improved vastus lateralis muscle atrophy (MuRF1, MAFbx), and increased protein synthesis (p70S6K) compared with those in the presarcopenia-MICT group. Taken together, these results indicate that lifelong exercise initiated in early adulthood in rats enhances autophagy activities and prevents skeletal muscle atrophy compared with the effects of no exercise or regular exercise initiated later in life.

MyomiRs are novel regulators of gene expression that can modulate many skeletal muscle processes, including myogenesis, regeneration, apoptosis, mitochondrial function, and aging-associated autophagy, which are involved in the conserved aging pathways (11,12). Consistent with previous reports, we found that aging altered miRNA expression profiles in skeletal muscle. In particular, the old-SED group exhibited a dysregulated miRNA expression profile compared with the adult-SED group, which may be associated with induced skeletal muscle atrophy upon aging (11–14,22,23). In addition, dysregulated HIPPO, MAPK, and PI3K/Akt signaling was found associated with altered expression of their members via specific miRNAs involved
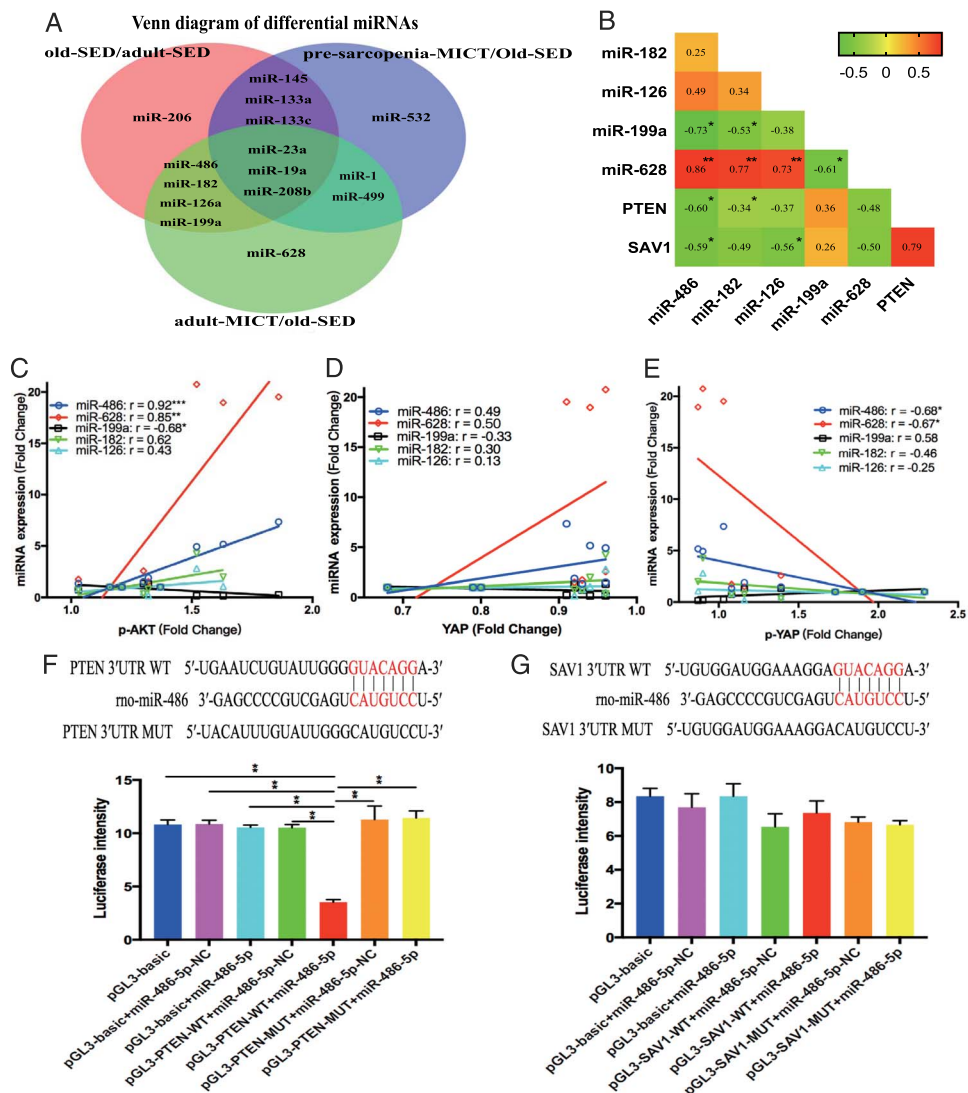
FIGURE 4—miR-486 directly targets PTEN but not SAV1. Venn diagram of differentially expressed miRNAs (A); correlation heat map (B); and correlation line graphs of p-Akt (C), YAP (D), and p-YAP (E). Luciferase reporter assays demonstrated that miR-486 targets PTEN (F) but not SAV1 (G). Groups: adult-SED, 8 months sedentary; old-SED, 26 months sedentary; adult-MICT, 8 months beginning with moderate-intensity continuous training; and presarcopenia-MICT, 18 months beginning with moderate-intensity continuous training.

in aging processes, which was accompanied by an increase in muscle atrophy and decrease in mitochondrial metabolism and biosynthesis, autophagy, and apoptosis markers.

In the present study, myomiR expression profiling of age skeletal muscle subjected to lifelong versus late-in-life endurance training identified five candidate miRNA targets of the PI3K/Akt pathway following adult-MICT protocol, including miRNA-486, miRNA-182, miRNA-126, miR-628, and miR-199a (Appendix, Supplemental Table 2, KEGG-enriched miRNAs and genes, http://links.lww.com/MSS/C304). In addition, we demonstrated that the adult-MICT regimen specifically enriched the expression of genes and proteins related to the PI3K/Akt pathway, which can prevent muscle fiber loss by regulating autophagy as well as protein degradation and skeletal muscle atrophy by inhibiting the expression of ubiquitinated protein ligases, such as MAFbx and MuRF1 (24). Notably, the increase in p70S6K, LC3II, and LC3II/LC3I, and decrease in MuRF1, MAFbx, and p62

expression observed in the adult-MICT rats compared with that in presarcopenia-MICT suggest that this regimen enhanced autophagy via myomiRs and PI3K/Akt/p70S6K signaling.

Notably, miR-486, which was specifically upregulated in the adult-MICT group, accounts for 21% of the total miRNA sequence reads in elderly skeletal muscle (25). miR-486, which is downregulated with age, not only functions as a biomarker of human muscle aging but also reflects the underlying molecular mechanisms of age-associated reduction in skeletal muscle mass (23). Moreover, miR-486 has been reported to activate Akt/FoxO signaling and improve skeletal muscle hypertrophy in animal models with chronic kidney disease–related muscular atrophy, myostatin knockout mice, hindlimb fixation-induced muscle atrophy, and Duchenne muscular dystrophy (26–29).

Our study results indicate that miR-486 is strongly correlated with the Akt pathway in the adult-MICT group, with
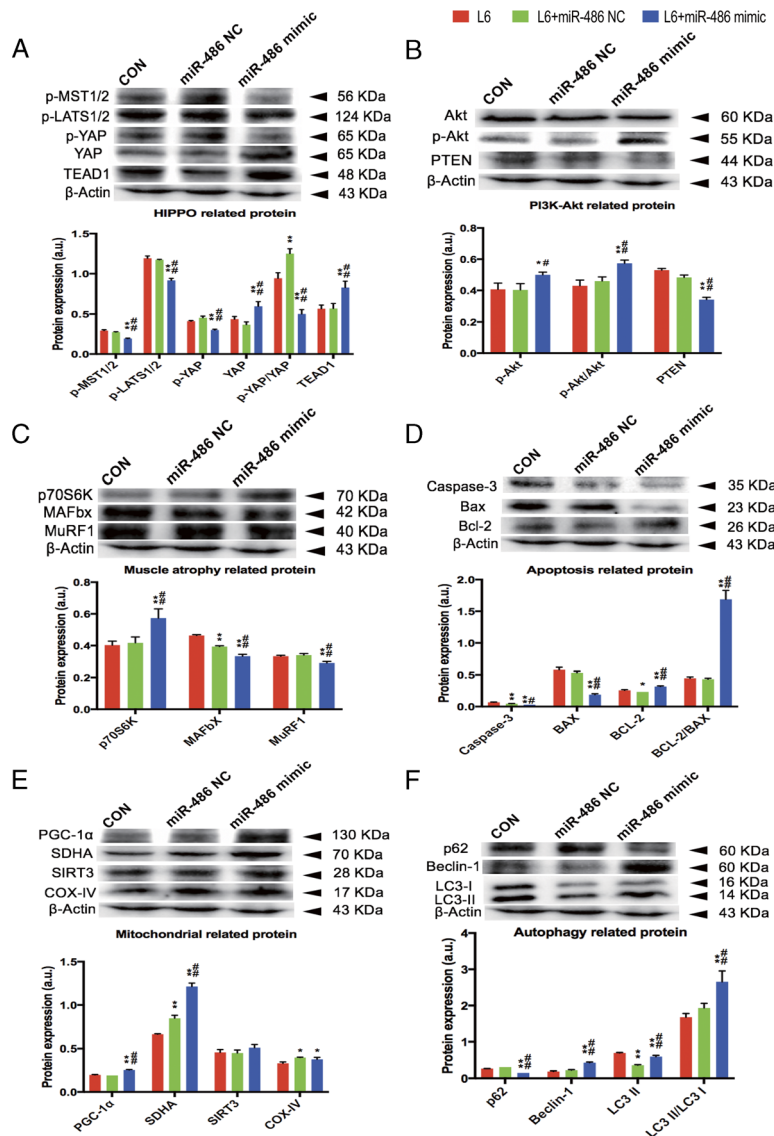
FIGURE 5—Expression of components involved in HIPPO (A) and PI3K/Akt (B) signaling, as well as muscle atrophy (C), apoptosis (D), mitochondrial function markers (E), and autophagy-related proteins (F). Values are reported as means ± SD. Groups: CON, L6 cells blank control; miR-486 NC, L6 cells + miR-486 NC; miR-486 mimic, L6 cells + miR-486 mimic. The CON, miR-486 NC, and miR-486 mimic groups were assessed via one-way ANOVA followed by Tukey's *post hoc* test. *$P < 0.05$ and **$P < 0.01$ vs CON; #$P < 0.05$ and ##$P < 0.01$ vs L6 + miR-486 NC.

respect to PTEN and p-Akt. Moreover, luciferase assays confirmed that PTEN, a negative regulator of PI3K/Akt signaling, is a direct target of miR-486 in L6 cells. Indeed, the inhibition of skeletal muscle atrophy and apoptosis, combined with the improved mitochondrial function and autophagy by the miR-486 mimic, correspond well with the inhibition of PTEN mRNA expression and increased p-Akt expression.

Interestingly, we also found that miR-486 was highly correlated with the HIPPO pathway in the adult-MICT group with respect to SAV1 and p-YAP. The HIPPO pathway is composed of three core component proteins: upstream MST1/2, midstream LATS1/2, and downstream YAP, and regulates tissue regeneration and organ size by controlling cell proliferation and differentiation (20). However, luciferase assays confirmed that SAV1, a positive regulator of HIPPO signaling, is not a direct target of miR-486 in L6 cells. These

findings are consistent with a previous study demonstrating that overexpressing miR-486 *in vitro* decreases PTEN expression, thereby activating PI3K/Akt signaling and indirectly inhibiting the canonical HIPPO pathway to promote nuclear localization of YAP and decreased p-YAP expression in response to mechanical stress and strain (30). Taken together, these results support the hypothesis that PTEN by miR-486 may be required for activating the PI3K/Akt pathway and indirectly inhibiting HIPPO signaling to improve aging skeletal muscle function.

Furthermore, nuclear localization of YAP regulates mitochondrial biogenesis (31) and directly promotes the expression of Armus (a RAB7-GAP required for autophagosome renewal) to increase autophagy flux, which plays an important role in tissue regeneration, autophagy fusion, and cell phenotypic plasticity (32). In the present study, overexpressing miR-486
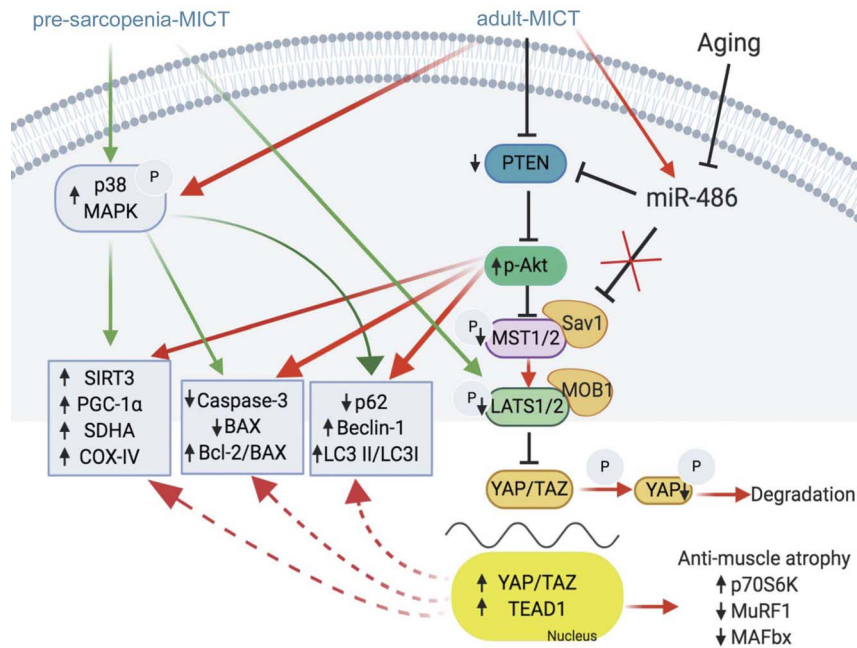
FIGURE 6—Summary of the possible mechanisms underlying the beneficial effects of lifelong regular exercise on muscle function. PTEN and p-Akt are the primary components of the PI3K/Akt pathway; p-MST1/2, p-LATS1/2, p-YAP, YAP, and TEAD1 are the main components of the HIPPO pathway. PTEN, phosphatase and tensin homolog; p-Akt, phosphorylated protein kinase B; p-MST1/2, phosphorylated mammalian ste-20 like kinase 1 and 2; p-LATS1/2, phosphorylated large tumor suppressor kinase 1 and 2; p-YAP, phosphorylated Yes-associated protein; TEAD1, TEA domain transcription factor 1.

in vitro increased marker expression of antiapoptotic proteins (Bcl-2/BAX ratio), mitochondrial function (SDHA and PGC-1α), autophagy (p62, Beclin-1 and LC3 II/LC3 I ratio), and protein synthesis (p70S6K), and prevented skeletal muscle atrophy (MAFbx and MuRF1), which may be related to the inhibition of HIPPO pathway (20). As shown in Figure 6, a possible mechanism that may be associated with effects elicited by the adult-MICT exercise regimen is the upregulation of miR-486, which targets PTEN and regulates PI3K/Akt and HIPPO signaling, and in turn enhances antiapoptosis protein expression, mitochondrial biogenesis, mitochondrial respiration, and autophagy to effectively delay skeletal muscle aging.

There are some limitations associated with this study. First, although the direct detection of myomiR expression profiles using quantitative RT-PCR has been previously validated (33), some data obtained via RNA sequencing may be omitted. Second, we reported data exclusively from the vastus lateralis muscle, and no comparison was performed with other muscle fiber types such as the extensor digitorum longus, tibialis anterior, or soleus muscle. In addition, our study was restricted to female rats, and thus, we cannot exclude differences based on sex.

CONCLUSIONS

Our findings demonstrated distinct differences in the protection against aging-related miRNA changes under adult-MICT and presarcopenia-MICT exercise regimens, as evidenced by KEGG analysis of differentially expressed miRNA. Specifically, the MAPK and HIPPO pathways were upregulated and downregulated, respectively, in both exercise groups, whereas the PI3K/Akt pathway was specifically upregulated in the adult-MICT group. Moreover, miR-486 directly targeted PTEN, activating the PI3K/Akt pathway and indirectly inhibiting the HIPPO pathway. When exercise was initiated at the beginning of adulthood, these observed changes led to a greater enhancement of mitochondrial function, antiapoptosis events, and autophagy and also increased protein synthesis and reduced skeletal muscle atrophy in age skeletal muscle.

REFERENCES

1. Wannamethee SG, Atkins JL. Muscle loss and obesity: the health implications of sarcopenia and sarcopenic obesity. *Proc Nutr Soc*. 2015; 74(4):405–12.
2. Kregel KC, Zhang HJ. An integrated view of oxidative stress in aging: basic mechanisms, functional effects, and pathological considerations. *Am J Physiol Regul Integr Comp Physiol*. 2007;292(1):R18–36.
3. Zampieri S, Pietrangelo L, Loefler S, et al. Lifelong physical exercise delays age-associated skeletal muscle decline. *J Gerontol A Biol Sci Med Sci*. 2015;70(2):163–73.
4. Koltai E, Bori Z, Osvath P, et al. Master athletes have higher miR-7, SIRT3 and SOD2 expression in skeletal muscle than age-matched sedentary controls. *Redox Biol*. 2018;19:46–51.

BASIC SCIENCES

5. Chambers TL, Burnett TR, Raue U, et al. Skeletal muscle size, function, and adiposity with lifelong aerobic exercise. *J Appl Physiol*. 2020;128(2):368–78.

6. Lavin KM, Perkins RK, Jemiolo B, Raue U, Trappe SW, Trappe TA. Effects of aging and lifelong aerobic exercise on basal and exercise-induced inflammation. *J Appl Physiol*. 2020;128(1):87–99.

7. Sailani MR, Halling JF, Møller HD, et al. Lifelong physical activity is associated with promoter hypomethylation of genes involved in metabolism, myogenesis, contractile properties and oxidative stress resistance in age human skeletal muscle. *Sci Rep*. 2019;9(1):3272.

8. Dethlefsen MM, Halling JF, Møller HD, et al. Regulation of apoptosis and autophagy in mouse and human skeletal muscle with aging and lifelong exercise training. *Exp Gerontol*. 2018;111:141–53.

9. Halling JF, Ringholm S, Olesen J, Prats C, Pilegaard H. Exercise training protects against aging-induced mitochondrial fragmentation in mouse skeletal muscle in a PGC-1α dependent manner. *Exp Gerontol*. 2017;96:1–6.

10. Gao HE, Wu DS, Sun L, et al. Effects of lifelong exercise on age-related body composition, oxidative stress, inflammatory cytokines, and skeletal muscle proteome in rats. *Mech Ageing Dev*. 2020;189:111262.

11. Brown DM, Goljanek-Whysall K. microRNAs: modulators of the underlying pathophysiology of sarcopenia? *Ageing Res Rev*. 2015;24:263–73.

12. Kirby TJ, Chaillou T, McCarthy JJ. The role of microRNAs in skeletal muscle health and disease. *Front Biosci (Landmark Ed)*. 2015;20:37–77.

13. Rivas DA, Lessard SJ, Rice NP, et al. Diminished skeletal muscle microRNA expression with aging is associated with attenuated muscle plasticity and inhibition of IGF-1 signaling. *FASEB J*. 2014;28(9):4133–47.

14. Zheng Y, Kong J, Li Q, Wang Y, Li J. Role of miRNAs in skeletal muscle aging. *Clin Interv Aging*. 2018;13:2407–19.

15. Russell AP, Wallace MA, Kalanon M, et al. Striated muscle activator of Rho signalling (STARS) is reduced in ageing human skeletal muscle and targeted by miR-628-5p. *Acta Physiol*. 2017;220(2):263–74.

16. Nair VD, Ge Y, Li S, et al. Sedentary and trained older men have distinct circulating exosomal microRNA profiles at baseline and in response to acute exercise. *Front Physiol*. 2020;11:605.

17. Li F-H, Sun L, Wu D-S, Gao H-E, Min Z. Proteomics-based identification of different training adaptations of age skeletal muscle following long-term high-intensity interval and moderate-intensity continuous training in age rats. *Aging (Albany NY)*. 2019;11(12):4159–82.

18. Vlachos IS, Zagganas K, Paraskevopoulou MD, et al. DIANA-miRPath v3.0: deciphering microRNA function with experimental support. *Nucleic Acids Res*. 2015;43(W1):W460–6.

19. Camera DM, Smiles WJ, Hawley JA. Exercise-induced skeletal muscle signaling pathways and human athletic performance. *Free Radic Biol Med*. 2016;98:131–43.

20. Gabriel BM, Hamilton DL, Tremblay AM, Wackerhage H. The Hippo signal transduction network for exercise physiologists. *J Appl Physiol*. 2016;120(10):1105–17.

21. Liang J, Zeng Z, Zhang Y, Chen N. Regulatory role of exercise-induced autophagy for sarcopenia. *Exp Gerontol*. 2020;130:110789.

22. Guo G, Gong L, Sun L, Xu H. Quercetin supports cell viability and inhibits apoptosis in cardiocytes by down-regulating miR-199a. *Artif Cells Nanomed Biotechnol*. 2019;47(1):2909–16.

23. Margolis LM, Lessard SJ, Ezzyat Y, Fielding RA, Rivas DA. Circulating microRNA are predictive of aging and acute adaptive response to resistance exercise in men. *J Gerontol A Biol Sci Med Sci*. 2017;72(10):1319–26.

24. Bonaldo P, Sandri M. Cellular and molecular mechanisms of muscle atrophy. *Dis Model Mech*. 2013;6(1):25–39.

25. Mitchell CJ, D'Souza RF, Schierding W, et al. Identification of human skeletal muscle miRNA related to strength by high-throughput sequencing. *Physiol Genomics*. 2018;50(6):416–24.

26. Alexander MS, Casar JC, Motohashi N, et al. MicroRNA-486–dependent modulation of DOCK3/PTEN/AKT signaling pathways improves muscular dystrophy–associated symptoms. *J Clin Invest*. 2014;124(6):2651–67.

27. Xu J, Li R, Workeneh B, Dong Y, Wang X, Hu Z. Transcription factor FoxO1, the dominant mediator of muscle wasting in chronic kidney disease, is inhibited by microRNA-486. *Kidney Int*. 2012;82(4):401–11.

28. Hitachi K, Nakatani M, Tsuchida K. Myostatin signaling regulates Akt activity via the regulation of miR-486 expression. *Int J Biochem Cell Biol*. 2014;47:93–103.

29. Zhu H-H, Wang X-T, Sun Y-H, et al. MicroRNA-486-5p targeting PTEN protects against coronary microembolization-induced cardiomyocyte apoptosis in rats by activating the PI3K/AKT pathway. *Eur J Pharmacol*. 2019;855:244–51.

30. Borreguero-Muñoz N, Fletcher GC, Aguilar-Aragon M, Elbediwy A, Vincent-Mistiaen ZI, Thompson BJ. The Hippo pathway integrates PI3K–Akt signals with mechanical and polarity cues to control tissue growth. *PLoS Biol*. 2019;17(10):e3000509.

31. Koo JH, Guan K-L. Interplay between YAP/TAZ and metabolism. *Cell Metab*. 2018;28(2):196–206.

32. Totaro A, Zhuang Q, Panciera T, et al. Cell phenotypic plasticity requires autophagic flux driven by YAP/TAZ mechanotransduction. *Proc Natl Acad Sci U S A*. 2019;116(36):17848–57.

33. Davidsen PK, Gallagher IJ, Hartman JW, et al. High responders to resistance exercise training demonstrate differential regulation of skeletal muscle microRNA expression. *J Appl Physiol*. 2011;110(2):309–17.